Supporting information

High-Entropy Single-Atom Catalysts via Spatial Confinement Synthesis for Oxygen Electrocatalysis and Zinc-Air Batteries

Xue Shen[1,‡], Zijian Li[2,‡], Haeseong Jang[3,*], Min Gyu Kim[4], Liqiang Hou[1,*], Xien Liu[1,*]

[1] State Key Laboratory of Advanced Optical Polymer and Manufacturing Technology, College of Chemical Engineering, Qingdao University of Science and Technology, Qingdao 266042, China

[2] Department of Chemistry, City University of Hong Kong, Hong Kong, SAR 999077, China

[3] Department of Advanced Materials Engineering, Chung-Ang University, Seoul 156-756, South Korea

[4] Beamline Research Division, Pohang Accelerator Laboratory (PAL), Pohang 37673, South Korea

* E-mail addresses: H. Jang, hjang4765@cau.ac.kr; L. Hou, houliqiang@qust.edu.cn; X. Liu, liuxien@qust.edu.cn

‡ X. S. and Z. L. contributed equally to this work.

Experimental Sections

Synthesis of DPCN: ZIF-8 was first synthesized by dissolving 1.118 g of $Zn(NO_3)_2 \cdot 6H_2O$ in 30 mL of methanol, and separately dissolving 1.232 g of 2-methylimidazole in another 30 mL of methanol. After magnetic stirring for 0.5 h, the two solutions were mixed and stirred continuously at room temperature for 24 h. The precipitate was collected by centrifugation, washed with methanol at least three times, and dried under vacuum at 70 °C for 10 h to obtain ZIF-8. The as-prepared ZIF-8 was then heated in a tube furnace at 900 °C for 3 h under an Ar/H_2 flow to yield DPCN. The resulting product was subsequently stirred in 0.5 M H_2SO_4 for 1 h, washed with deionized water until the supernatant reached neutral pH, collected again by centrifugation, and dried to obtain the final DPCN support.

Synthesis of HESAC: A mixture of metal acetylacetonate precursors—$Co(acac)_2$ (10.5 mg), $Fe(acac)_3$ (8.83 mg), $Cu(acac)_2$ (6.54 mg), $Mn(acac)_3$ (8.81 mg), and $Ni(acac)_2$ (6.42 mg)—was dissolved in 20 mL of a water–ethanol mixed solvent. Then, 145 mg of DPCN was dispersed into the above solution and ultrasonicated for 0.5 h. The suspension was heated at 70 °C under magnetic stirring to evaporate the solvent, forming a thick slurry, which was then fully dried. The resulting solid was ground thoroughly in an agate mortar. The powder was subsequently annealed at 800 °C for 4 h under a flowing Ar/NH_3 atmosphere. After cooling, the product was treated with 0.1 M $HClO_4$ for 0.5 h, collected by centrifugation, washed thoroughly, and dried to obtain the final HESAC material.

XC-72-supported control: Commercial XC-72 carbon was first calcined at 300 °C for 3 h under Ar flow to remove surface impurities. Subsequently, 48.3 mg of the treated XC-72 and the same molar amounts of acetylacetonate salts of Mn, Fe, Co, Ni, and Cu as used in the HESAC synthesis were dispersed in 100 mL of a water-ethanol (1:1 v/v) mixture by ultrasonication for 30 min. The suspension was stirred at 70 °C to evaporate the solvent, and the resulting slurry was dried and ground in an agate mortar. The powder was then annealed at 800 °C for 4 h under Ar/NH_3 (95:5 v/v), followed by acid washing (0.1 M $HClO_4$, 30 min), centrifugation, washing, and drying to obtain the first control sample.

Chloride-precursor control: 48.3 mg of DPCN and the same molar amounts of metal chloride precursors ($MnCl_2$, $FeCl_3$, $CoCl_2$, $NiCl_2$, $CuCl_2$) as the corresponding acetylacetonates were dispersed in 100 mL of a water-ethanol (1:1 v/v) mixture via 30 min ultrasonication. After solvent removal at 70 °C under stirring, the dried solid was ground and subjected to the same thermal treatment (800 °C, 4 h, Ar/NH_3), acid washing, and workup procedure as described above, yielding the second control sample.

Materials Characterization: The crystalline structures of the as-prepared samples were determined by X-ray diffraction (XRD) on a Bruker D8 ADVANCE diffractometer equipped with Cu Kα radiation (λ = 1.5418 Å). Data were collected in the 2θ range of 10–80° at a scanning speed of 10° min^{-1}. Morphological and microstructural analyses were performed using a JEOL JEM-2100F transmission electron microscope (TEM) and a FEI Quanta200F scanning electron microscope (SEM), operated at 200 kV and under standard conditions, respectively. Nitrogen sorption isotherms were measured at 77 K using a Micromeritics ASAP 2020 system. The specific surface area was calculated using the Brunauer–Emmett–Teller (BET) method, while pore size distribution and pore volume were derived using density functional theory (DFT) models. Raman spectra were acquired on a Renishaw in Via confocal Raman microscope with a 532 nm laser excitation source. X-ray absorption spectroscopy (XAS) measurements at the Mn, Fe, Co, Ni, and Cu K-edges were conducted in fluorescence mode at the 1W1B beamline of the Beijing Synchrotron Radiation Facility (BSRF). The acquired XAS data were processed and fitted using the Demeter software package (Athena and Artemis modules).

Electrochemical Measurements: The electrocatalytic activities for the oxygen reduction reaction (ORR) were evaluated in a standard three-electrode electrochemical cell. A glassy carbon electrode (4 mm diameter) served as the working electrode, a Pt wire as the counter electrode, and a Hg/HgO electrode as the reference electrode. All potentials were converted to the reversible hydrogen electrode (RHE) scale using the following calibration: E (RHE) = E (Hg/HgO) + 0.0591 × pH + 0.098. The

catalyst ink was prepared by ultrasonically dispersing 2 mg of catalyst in a mixture containing 0.1 mL ultrapure water, 0.2 mL ethanol, and 40 μL of 5 wt% Nafion solution. A 5 μL aliquot of the ink was drop-cast onto the glassy carbon surface and dried to form a uniform catalyst layer. The electrolyte (0.1 M KOH) was saturated with oxygen by purging for 20 min prior to measurements, and the O_2 atmosphere was maintained throughout the tests. For comparison, commercial 20 wt% Pt/C was evaluated under identical conditions. The oxygen evolution reaction (OER) performance was assessed in a three-electrode configuration with a carbon rod as the counter electrode and an RHE as the reference. The working electrode was prepared by depositing 5 μL of a homogenously dispersed catalyst ink (prepared via ultrasonic dispersion) onto a glassy carbon disk (geometric area: 0.07065 cm^2). Linear sweep voltammetry (LSV) was performed from 1.0 to 2.0 V vs. RHE in 1 M KOH electrolyte.

Zinc-Air Battery Assembly and Testing: Air cathodes were fabricated by coating a slurry of activated charcoal and polytetrafluoroethylene (PTFE) binder (weight ratio of 7:3) onto nickel foam substrates. The electrode thickness was controlled to approximately 700 μm using a rolling press. To prepare the catalyst layer, 10 mg of the catalyst was dispersed in a solution containing 0.25 mL ethanol and 200 μL of 5 wt% Nafion solution via sonication. The resulting homogeneous ink (200 μL) was uniformly applied onto the pre-formed gas diffusion layer and dried under vacuum for 30 min, followed by mild pressing to ensure adhesion. Both primary and rechargeable zinc-air batteries were assembled using the as-prepared catalyst-coated air cathodes. A polished zinc plate was employed as the anode, separated from the cathode by a nylon polymer membrane. The assembly was infused with 6 M KOH solution as the electrolyte, and nickel foam was used as the current collector for both electrodes.

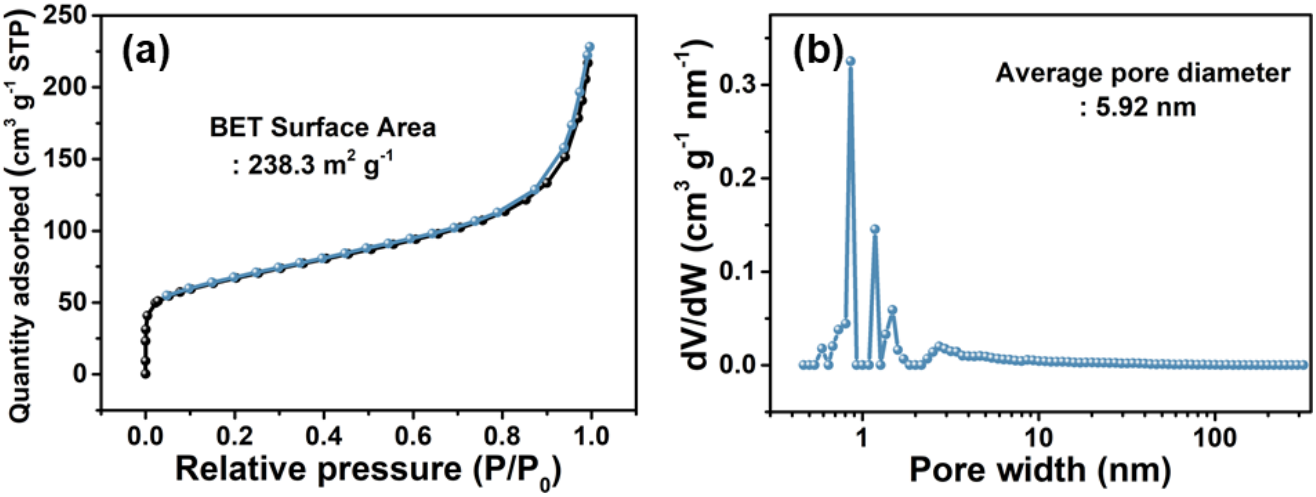

Fig. S1. (a) Nitrogen adsorption-desorption isotherm and (b) pore-size distribution of XC-72.

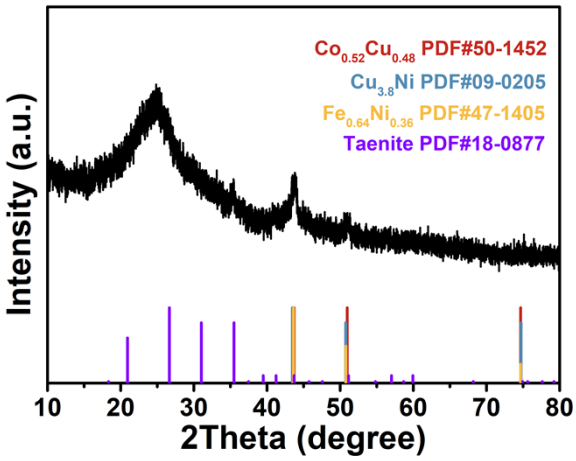

Fig. S2. XRD pattern of the sample prepared using XC-72 carbon as the support under otherwise identical HESAC synthesis conditions..

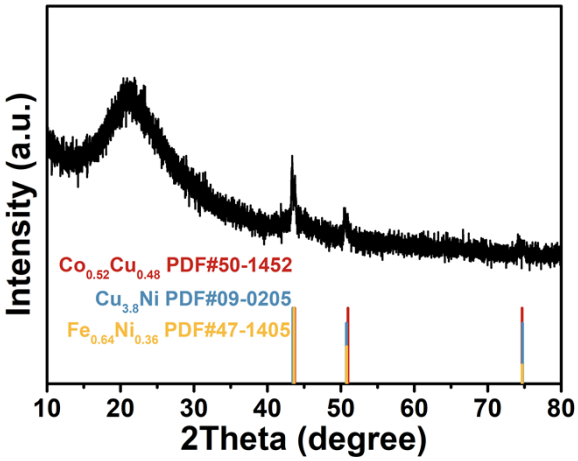

Fig. S3. XRD pattern of the sample synthesized using metal chloride precursors instead of acetylacetonates with the DPCN support.

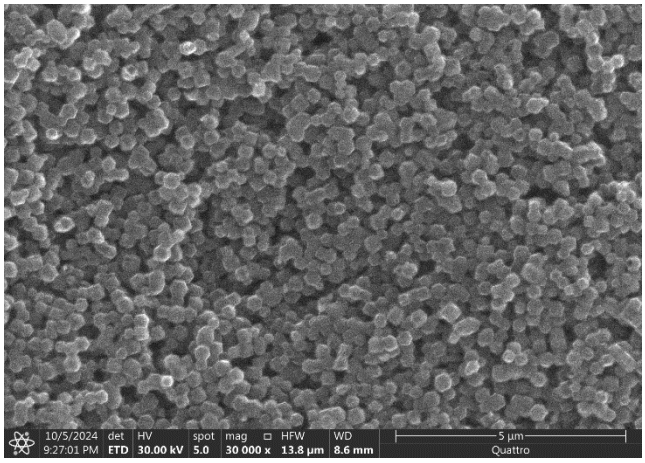

Fig. S4. SEM image of HESAC.

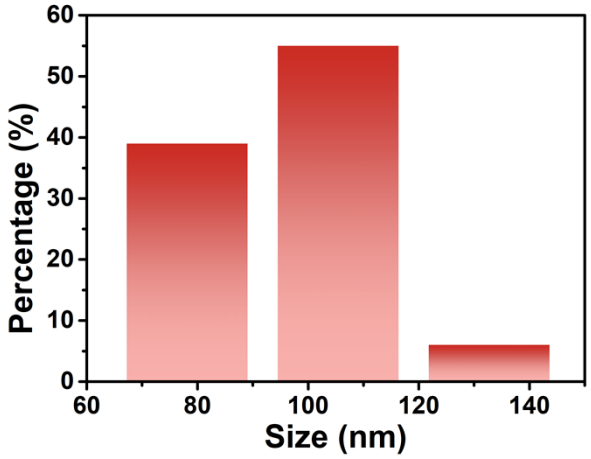

Fig. S5. Histogram of the particle size distribution for HESAC.

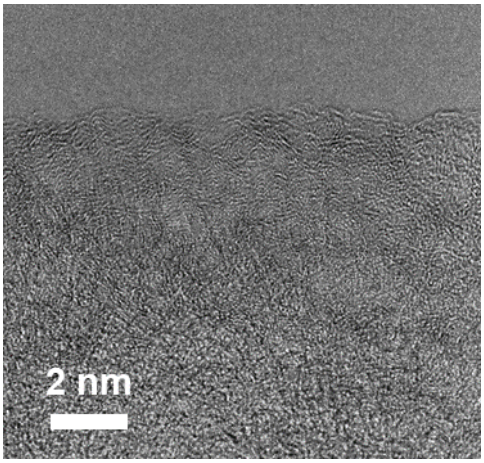

Fig. S6. HRTEM image of HESAC.

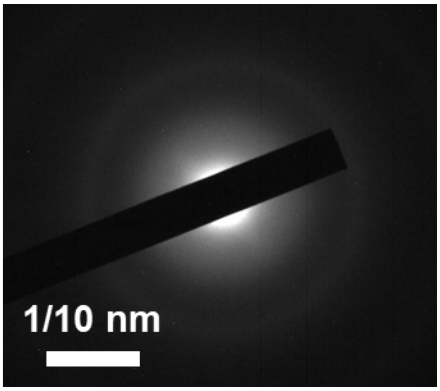

Fig. S7. SAED Pattern of HESAC.

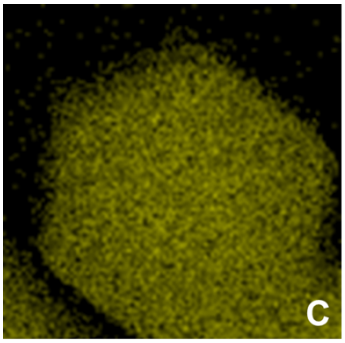

Fig. S8. Elemental Mapping of HESAC.

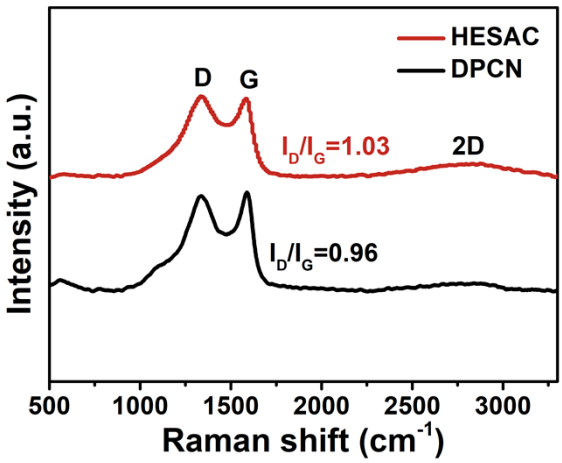

Fig. S9. Raman spectra of the DPCN support and the final HESAC catalyst.

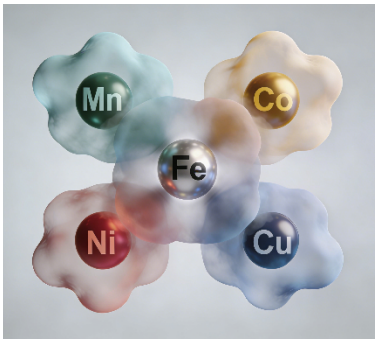

Fig. S10. Schematic diagram for the "cocktail effect".

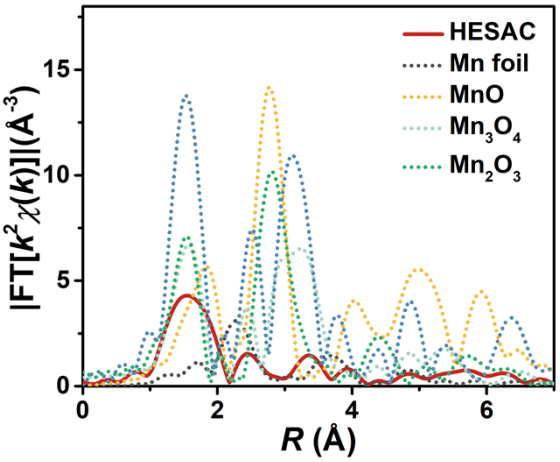

Fig. S11. Fourier-transform Mn K-edge EXAFS spectra.

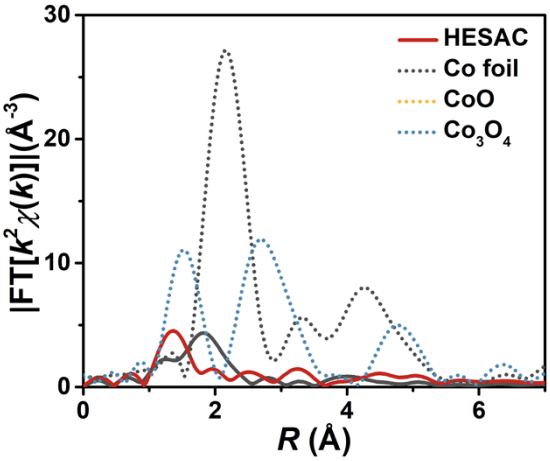

Fig. S12. Fourier-transform Co K-edge EXAFS spectra.

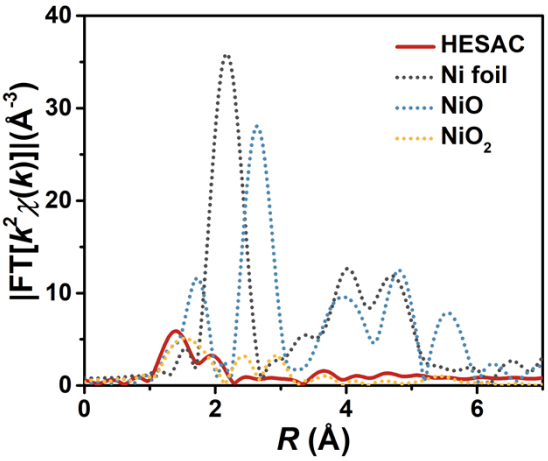

Fig. S13. Fourier-transform Ni K-edge EXAFS spectra.

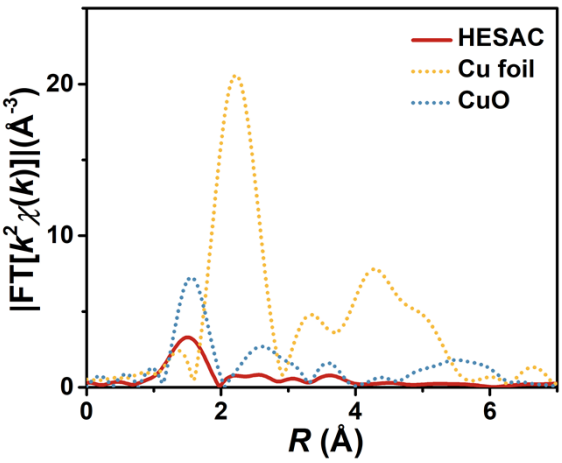

Fig. S14. Fourier-transform Cu K-edge EXAFS spectra.

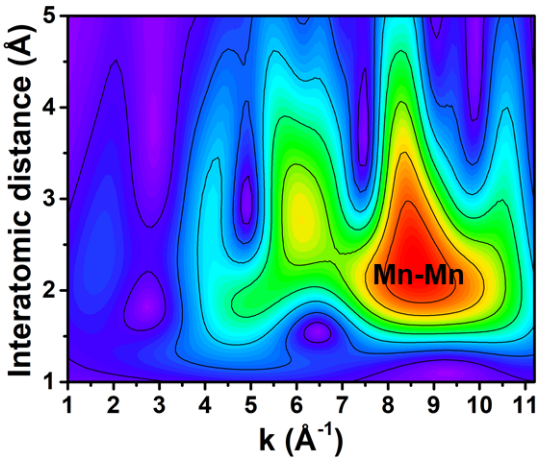

Fig. S15. Wavelet transform plots of the EXAFS for Mn in Mn foil.

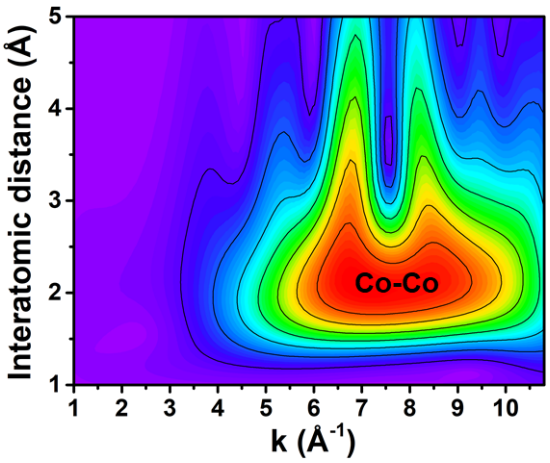

Fig. S16. Wavelet transform plots of the EXAFS for Co in Co foil.

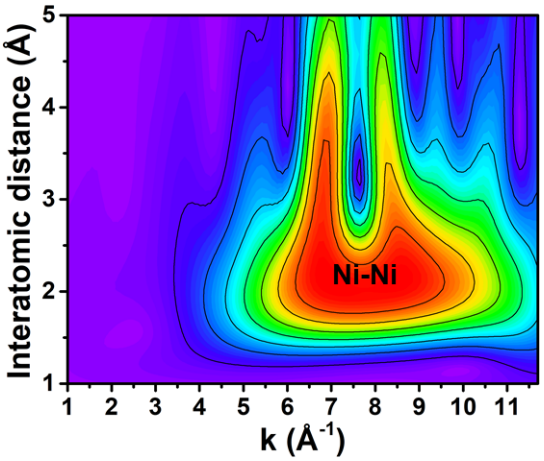

Fig. S17. Wavelet transform plots of the EXAFS for Ni in Ni foil.

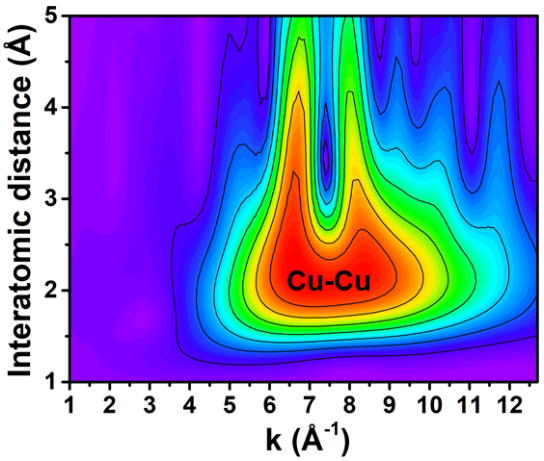

Fig. S18. Wavelet transform plots of the EXAFS for Cu in Cu foil.

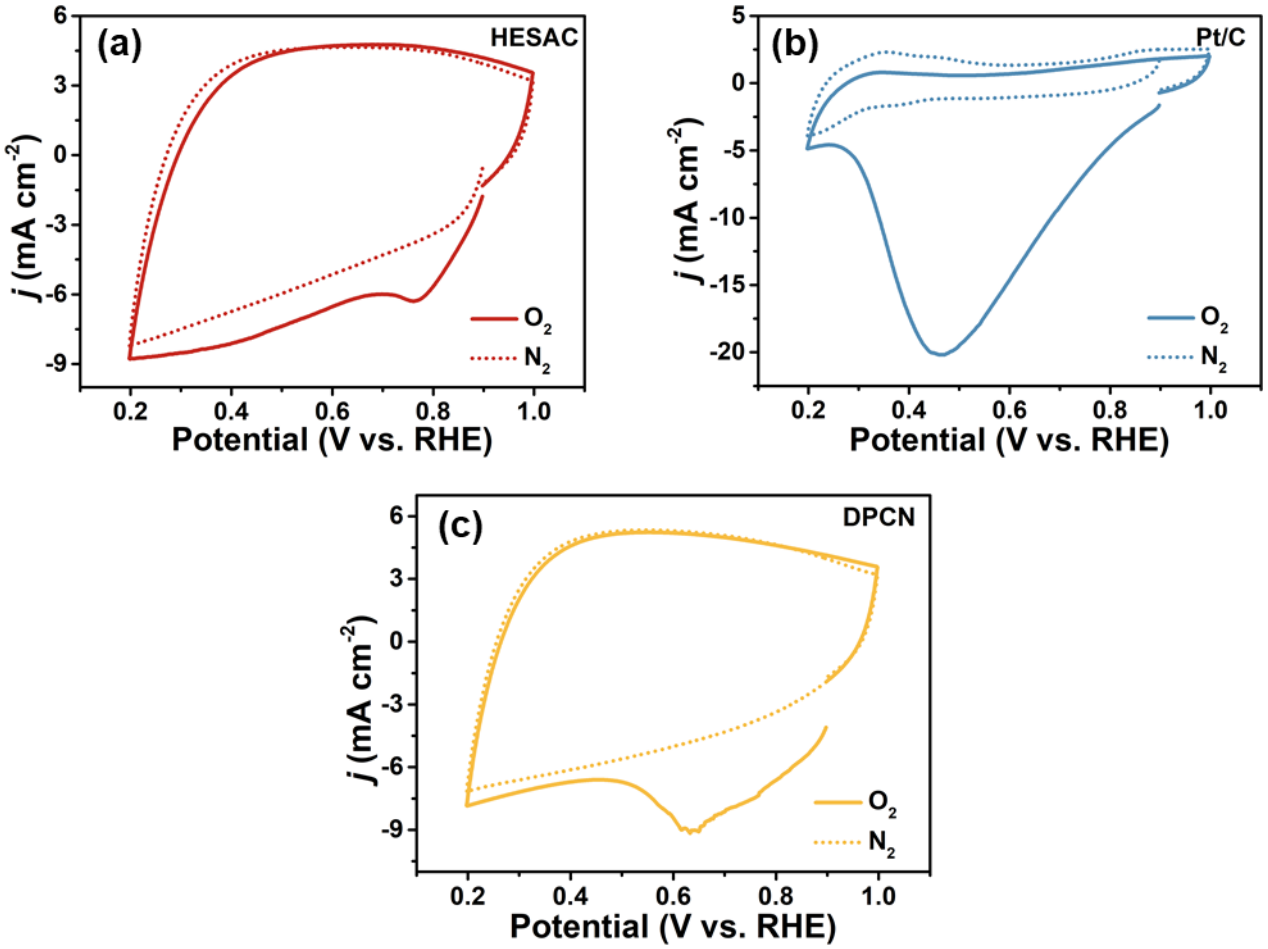

Fig. S19. CV curves of (a) HESAC, (b) Pt/C, and (c) DPCN in 0.1 M KOH during ORR.

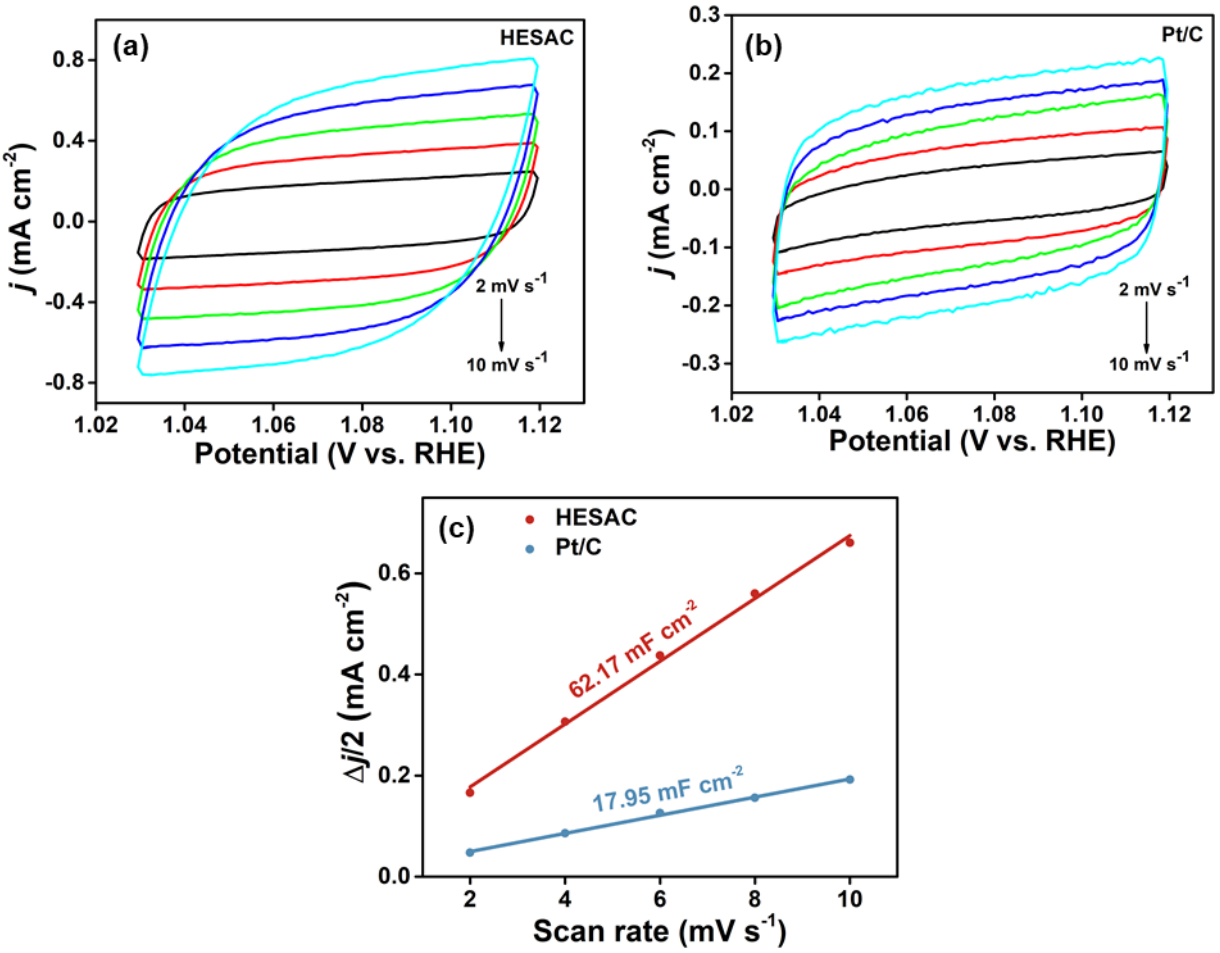

Fig. S20. Cyclic voltammetry curves at various scan rates ranging from 2 to 10 mV s^{-1} within the non-Faradaic electrode potential range in 0.1 M KOH for (a) HESAC (b) Pt/C. (c) Electrochemical active surface area (ECSA) of HESAC and Pt/C.

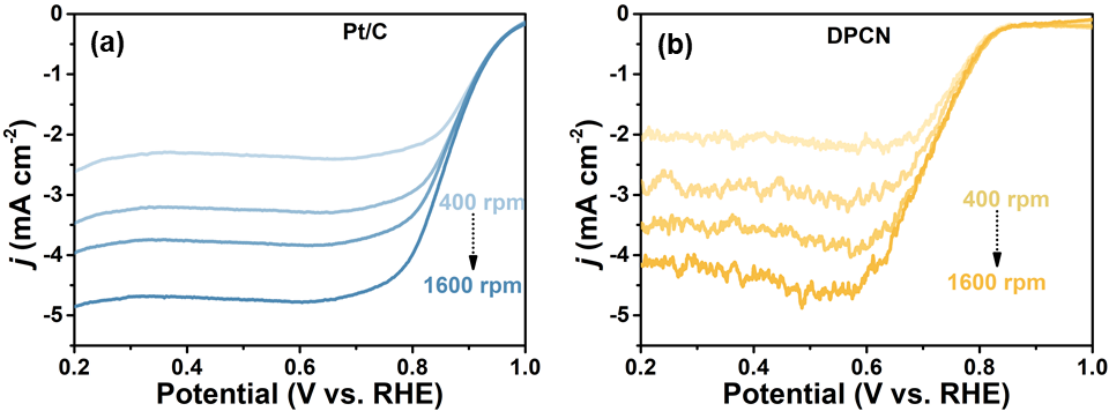

Fig. S21. ORR polarization curves at different rotation speeds for (a) Pt/C and (b) DPCN.

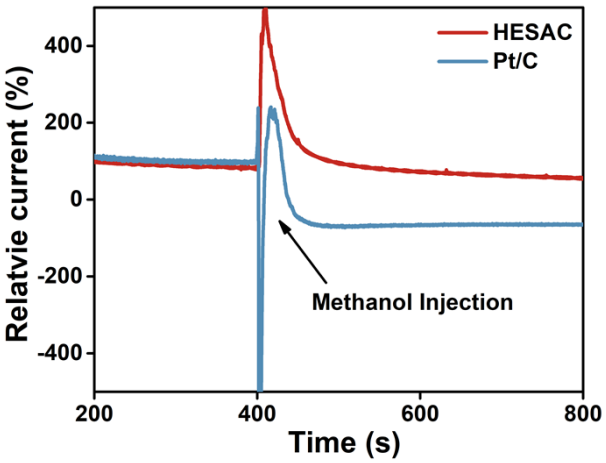

Fig. S22. Methanol resistance i–t test of HESAC and Pt/C.

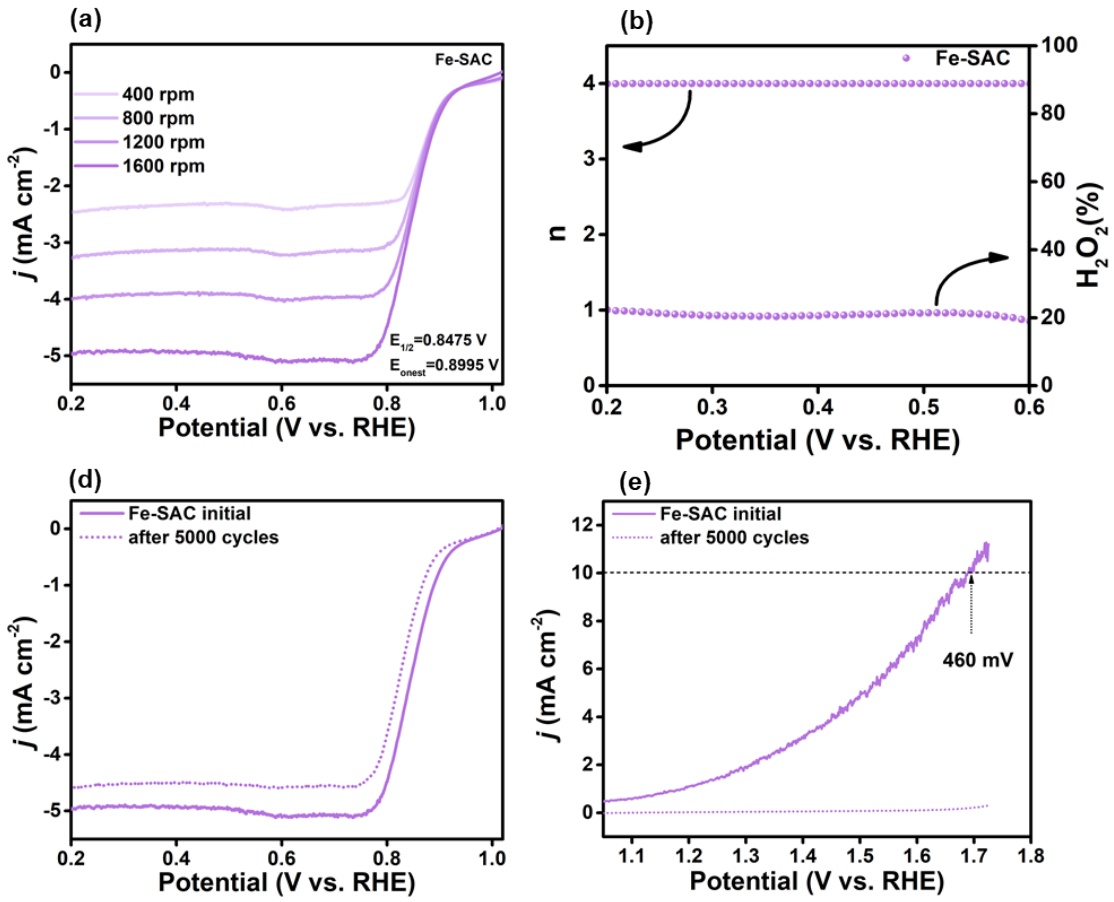

Fig. S23. (a) ORR polarization curves of Fe-SAC at different rotation speeds. (b) H_2O_2 yield and electron transfer number obtained from RRDE measurements. (c) Comparison of ORR polarization curves for Fe-SAC before and after 5000 cycles of accelerated durability testing. (d) OER polarization curves for Fe-SAC before and after 5000 cycles of accelerated durability testing.

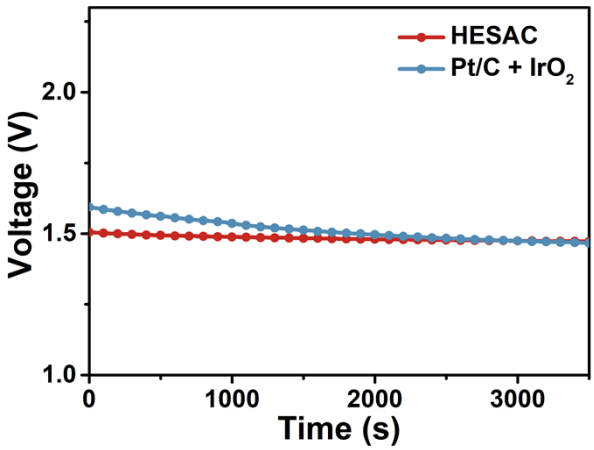

Fig. S24. Open-circuit voltage of ZABs based on HESAC and Pt/C+IrO_2.

Table S1. ICP-OES data for five elements.

Element	Mn	Fe	Co	Ni	Cu
Mass fraction (wt%)	0.21	0.19	0.40	0.38	0.30